

Radical Reactions

Deutsche Ausgabe: DOI: 10.1002/ange.201508922
Internationale Ausgabe: DOI: 10.1002/anie.201508922

Bent Carbon Surface Moieties as Active Sites on Carbon Catalysts for Phosgene Synthesis

Navneet K. Gupta, Anastasia Pashigreva, Evgeny A. Pidko,* Emiel J. M. Hensen, Leslaw Mleczko, Stefan Roggan,* Erika E. Ember,* and Johannes A. Lercher*

Abstract: Active sites in carbon-catalyzed phosgene synthesis from gaseous CO and Cl₂ have been identified using C₆₀ fullerene as a model catalyst. The carbon atoms distorted from sp² coordination in non-planar carbon units are concluded to generate active Cl₂. Experiments and density functional theory calculations indicate the formation of a surface-bound [C₆₀⋯Cl₂] chlorine species with radical character as key intermediate during phosgene formation. It reacts rapidly with physisorbed CO in a two-step Eley–Rideal-type mechanism.

The synthesis of phosgene (COCl₂) by a catalyzed reaction between gaseous chlorine (Cl₂) and carbon monoxide (CO) is one of the oldest, most reliable, and efficient large-scale chemical processes.^[1] Since catalytic COCl₂ synthesis has replaced earlier processes based on photolysis,^[2] the activated carbon used as catalyst has remained basically unchanged. While several kinetic studies on phosgene formation have been reported,^[3] mechanistic insight into carbon-catalyzed COCl₂ synthesis and the associated active sites is largely lacking.^[4] This may in part be associated with the diversity and chemical complexity of carbon surface structures rendering the identification of the active sites on carbon catalysts highly challenging.

To initiate the development of a new generation of stable and highly active catalysts, the nature of active sites and of the elementary steps of COCl₂ synthesis from CO and Cl₂ on activated carbon have been studied. Insight is critical not only to optimize catalytic properties by maximizing the concen-

tration of active sites, but also to minimize production of chlorinated side products.

In a first step, transmission electron microscopy has been used to exemplify the characteristic features of a typical activated carbon catalyst, that is, the ample presence of bent carbon layers, semi-spheres, and carbon cages (Figure 1). Bending of the carbon structures is usually induced by the presence of 5-membered rings or the combination of 5- and 7-membered rings (Stone–Wales defects).^[5]

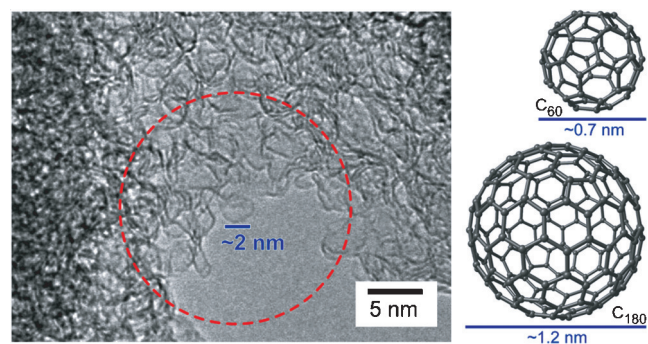


Figure 1. HR-TEM image of an activated carbon catalyst for COCl₂ synthesis from CO and Cl₂ showing curled carbon layers (left) and carbon semi-spheres that resemble fullerene-type structures (right).

The diameters of these bent structural units (Figure 1, blue bar) approximate the diameter of fullerenes, which range from 0.71 (C₆₀) to 1.2 nm (C₁₇₆).^[6,7] The structural analogy between the curved surfaces of activated carbon and the molecular structure of fullerenes stimulated us, in consequence, to select fullerenes as well-defined model catalysts. These models lack defect sites, edges, and functional groups. It allows the mechanism of carbon-catalyzed Cl₂ activation and conversion with CO to be explored in the absence of various more reactive but less defined carbon species.

Table 1 compares DFT-computed reaction energies for COCl₂ formation and the Cl₂ addition to unsaturated moieties in several model structures with distinct structural characteristics, that is, a planar C₃₂H₁₄ graphene model, 2-butene, and C₆₀. Only in the case of C₆₀, the reaction energy is lower than that of the reaction of Cl₂ with CO. The reaction of Cl₂ with graphene is highly endothermic, and addition to graphene has not been observed.^[8] Chlorination of butene is strongly exothermic, suggesting the formation of strong and stable C–Cl bonds. We hypothesize, therefore, that the curved structure of the conjugated fullerene π -system provides the appropriate balance between the loss of conjugation energy

* N. K. Gupta, Dr. A. Pashigreva, Dr. E. E. Ember, Prof. J. A. Lercher
Technische Universität München, Department of Chemistry and
Catalysis Research Center
Lichtenbergstrasse 4, 85748 Garching (Germany)
E-mail: erika.ember@mytum.de
johannes.lercher@ch.tum.de

Dr. E. A. Pidko, Prof. E. J. M. Hensen
Laboratory of Inorganic Materials Chemistry, Schuit Institute of
Catalysis, Eindhoven University of Technology
PO Box 513, 5600 MB Eindhoven (The Netherlands)

Dr. E. A. Pidko
Institute for Complex Molecular Systems
Eindhoven University of Technology
PO Box 513, 5600 MB Eindhoven (The Netherlands)
E-mail: e.a.pidko@tue.nl

Prof. L. Mleczko, Dr. S. Roggan
Technology Development, Bayer Technology Services GmbH
51368 Leverkusen (Germany)
E-mail: stefan.roggan@bayer.com

Supporting information and ORCID(s) from the author(s) for this article are available on the WWW under <http://dx.doi.org/10.1002/anie.201508922>.

Table 1: DFT-computed reaction enthalpies (B3LYP-D3/TZVP//6-31G-(d,p)) of Cl_2 addition via $\text{X} + \text{Cl}_2 \rightarrow \text{XCl}_2$.

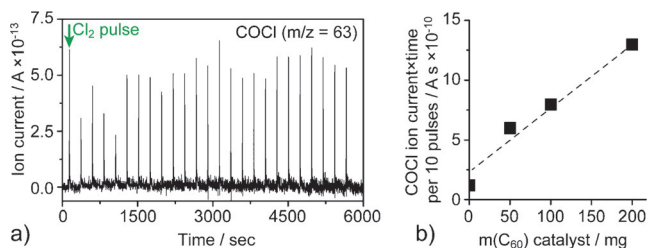
X	Graphene ^[a]	C_{60}	CO ^[b]	2-Butene ^[b]
ΔH_r [kJ mol ⁻¹]	+227	-18	-124	-189

[a] The structure of graphene was approximated by a $\text{C}_{32}\text{H}_{14}$ fragment in this calculation (see the Supporting Information for further details).

[b] The experimental ΔH_r values for CO and 2-butene chlorination are -109.6 and -191.2 kJ mol⁻¹, respectively.^[1e]

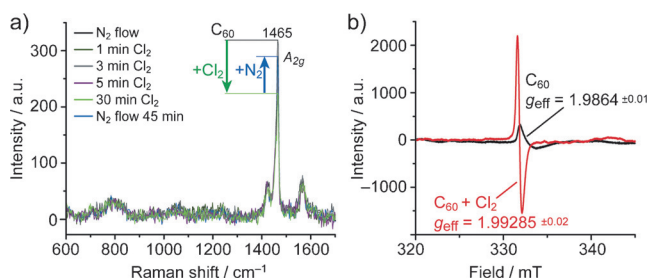
and the energy gain in reactive coordination of Cl_2 (Supporting Information, Figure S1), in line with the relatively low exothermicity of Cl_2 addition to C_{60} .

To test the suitability of C_{60} as a model catalyst for COCl_2 synthesis, the material was exposed to CO and Cl_2 pulses at 200 °C (Supporting Information, Figure S2). Once the reversible adsorption of Cl_2 was established, the stable catalytic formation of COCl_2 was detected by online mass-spectrometry ($m/z = 63$, Figure 2a), corresponding to $[\text{COCl}]^+$. Without catalyst, only negligible concentrations of COCl_2 formed (Figure 2b).

**Figure 2.** a) COCl_2 formation on applying Cl_2 pulses over solid C_{60} at 200 °C in 5% CO in He. b) Comparison of the COCl_2 formation in the presence of various amounts of C_{60} fullerene.

To probe the hypothesis that Cl_2 has to be weakly adsorbed to be successfully activated and converted into COCl_2 , in situ Raman spectroscopy was used to study the interaction of Cl_2 with the C_{60} fullerene (Figure 3a). The pentagonal pinch mode A_{2g} at 1465 cm^{-1} was used to monitor the electronic environment of the carbon atoms.^[8–10]

In the presence of Cl_2 , the intensity of the A_{2g} band decreased, rapidly reaching a new equilibrium (Figure 3a). Purging with an inert gas reverted the spectral changes

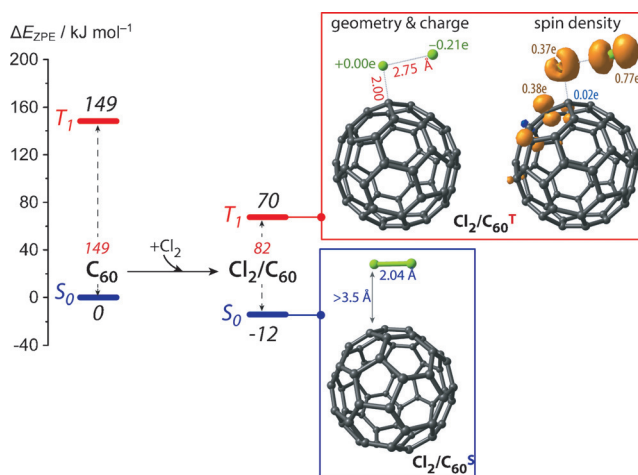
**Figure 3.** a) In situ Raman spectra of C_{60} contacted with Cl_2 at 40 °C. b) Comparison of the ESR spectra of C_{60} under inert conditions (black) and in a Cl_2 atmosphere (red) recorded at ambient temperature.

induced by Cl_2 addition. This demonstrates a reversible interaction between Cl_2 and C_{60} involving the formation of a $[\text{C}_{60} \cdots \text{Cl}_2]$ complex, presumably via a charge transfer from C_{60} to Cl_2 .^[11] Reduction of the spherical symmetry upon C–Cl bond formation eliminates the A_{2g} band and results in new Raman bands at 650–850 cm^{-1} (C–Cl vibration in $\text{C}_{60}\text{Cl}_{30}$; Supporting Information, Figure S3a). Combined Raman (Figure 3a) and elemental analysis (Supporting Information, Table S1) of the Cl_2 treated C_{60} further show that the $[\text{C}_{60} \cdots \text{Cl}_2]$ interaction has neither led to the formation of covalent C–Cl bonds nor significantly changed the symmetry of fullerene.

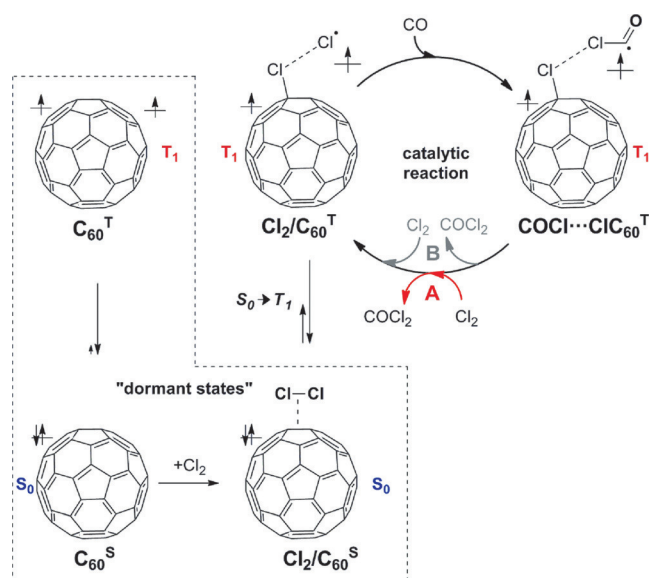
To characterize the reversibly adsorbed $[\text{C}_{60} \cdots \text{Cl}_2]$ species, ESR spectroscopy was used (Figure 3b). Neutral C_{60} has no unpaired electrons and is, therefore, ESR-inactive. However, in our studies an ESR signal at $g = 1.9864 \pm 0.01$ was observed for the nominally neutral C_{60} due to the presence of small amount (5.4×10^{17} spin g^{-1}) of paramagnetic defects generated during the synthesis procedure or the purification. The ESR line patterns indicate that these defects are delocalized over all the C atoms of the C_{60} cage, so that the contributions to the ESR line are dynamically averaged over all sites on C_{60} .^[12] Upon Cl_2 exposure, a new strong signal was observed at $g_{\text{eff}} = 1.9928 \pm 0.02$ indicating the localized Cl_2 adsorption and formation of strong paramagnetic $[\text{C}_{60} \cdots \text{Cl}_2]$ charge-transfer complex.^[12] The singlet line, an isotropic doublet without zero-field splitting peaks, indicates that the symmetry of the C_{60} fullerene cage was not changed by exohedral functionalization.

DFT calculations were performed to rationalize these experimental observations. Figure 4 shows the calculated reaction energy diagram for the activation of Cl_2 in the presence of C_{60} .

The activation of Cl_2 by C_{60} leading to $\text{C}_{60}/\text{Cl}_2^{\text{S}}$ in the ground singlet state (S_0) proceeds with a prohibitively high-energy barrier (exceeding 400 kJ mol⁻¹, as estimated by relaxed potential energy scan calculations). Therefore, we

**Figure 4.** Reaction energy diagram and optimized structures (selected bond lengths are given in Å, Mulliken atomic charges and spin density are given for the open-shell Cl_2 adsorption complex $\text{Cl}_2/\text{C}_{60}^{\text{T}}$) of intermediates involved in Cl_2 adsorption and activation by C_{60} in the singlet (S_0) and triplet (T_1) electronic configurations.

conclude that a direct activation of Cl_2 on a C_{60} in the singlet state is not possible in the reaction space explored. Cl_2 activation becomes favorable when the reaction proceeds over the triplet excited potential energy surface. DFT-computed energy differences between the singlet (S_0) and triplet (T_1) electron configurations of C_{60} is 149 kJ mol^{-1} , that is, in excellent agreement with the reported experimental values ($150\text{--}155 \text{ kJ mol}^{-1}$).^[13,14] In the presence of Cl_2 , the triplet electronic configuration (T_1 , Figure 4, $\text{Cl}_2/\text{C}_{60}^T$) becomes strongly stabilized and is only 70 kJ mol^{-1} higher in energy than the respective ground state of a Cl_2 and C_{60} mixture. The T_1 adsorption complex $\text{Cl}_2/\text{C}_{60}^T$ can be regarded as a biradical species featuring a Cl radical anion coupled with the C_{60}Cl unit in which the spin density is delocalized, as shown in Figure 4. This is in line with the ESR spectra (Figure 3), showing the formation of Cl_2 radicals when Cl_2 is adsorbed on C_{60} . Such radical $\text{Cl}_2/\text{C}_{60}^T$ species are hypothesized to be the key species for the catalytic conversion of CO to COCl_2 . DFT calculations indicate a very favorable catalytic



Scheme 1. Proposed mechanism for $\text{Cl}_2/\text{C}_{60}^T$ catalyzed COCl_2 formation following an Eley–Rideal mechanism. The potentially dormant off-cycle species are shown in the dashed rectangle, while alternative paths for the regeneration of the catalytic species $\text{Cl}_2/\text{C}_{60}^T$ are indicated as paths A and B.

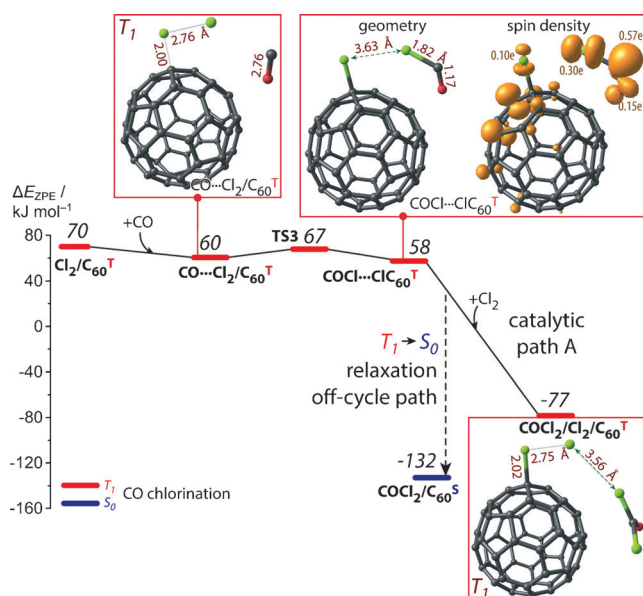


Figure 5. Reaction energy diagram and structures of key intermediates and transition states involved in phosgene synthesis over C_{60} .

path (Figure 5, Scheme 1). The cycle starts with the facile reaction ($E_{\text{act}} = 7 \text{ kJ mol}^{-1}$) of CO with a Cl radical moiety of $\text{Cl}_2/\text{C}_{60}^T$ yielding COCl^\cdot ($\text{CO}\cdots\text{Cl}_2/\text{C}_{60}^T \rightarrow \text{COCl}\cdots\text{ClC}_{60}^T$, Figure 5). The favorable path proceeds via a barrierless reaction of COCl^\cdot with another Cl_2 to yield COCl_2 (Figure 5) and regenerate $\text{Cl}_2/\text{C}_{60}^T$ (Scheme 1, path A). However, the direct recombination of the COCl^\cdot and adjacent Cl^\cdot radicals (Scheme 1, path B) resulting in COCl_2 and transient C_{60}^T that is readily stabilized by Cl_2 to form $\text{Cl}_2/\text{C}_{60}^T$ also cannot be completely ruled out. The off-cycle spin-crossing $T_1 \rightarrow S_0$ relaxation path (Figure 5) is less likely and would give a catalytic cycle with an apparent activation energy E_{act} over 70 kJ mol^{-1} needed for the transition to the active T_1 state (Figure 4). This is in a strong contrast to the observed barrier of 18 kJ mol^{-1} (Supporting Information, Table S2).

The proposed reaction sequence is in line with the observed reaction order of one (Supporting Information, Table S2) in Cl_2 and CO . The apparent activation energy was significantly lower (18 kJ mol^{-1}) than that measured for an activated carbon catalyst (56 kJ mol^{-1} ; Supporting Information, Table S2),^[3] clearly indicating the subtle effect of the local environment of the active sites on the structure and energy of the transition state. At this point, we would like to stress that the proposed active site, the triplet $[\text{Cl}_2\cdots\text{C}_{60}]$ will increase in concentration with temperature, as it lies 70 kJ mol^{-1} higher than the ground state of isolated C_{60} and Cl_2 .

To independently probe the presence of radicals, $[\text{C}_{60}\cdots\text{Cl}_2]$ was reacted with CH_4 , which is known to be chlorinated by radical substitution. The reaction led to a mixture of CH_3Cl , CH_2Cl_2 , and CHCl_3 . In presence of C_{60} a five-fold rate increase compared to the non-catalytic thermal chlorination of CH_4 was observed at 200°C (Figure 6) evidencing unequivocally the presence of surface-bound Cl^\cdot radicals.

Thus, combining ESR and Raman spectroscopic analysis and reactivity data, we conclude that a reversible surface bound radical $[\text{C}_{60}\cdots\text{Cl}_2]$ species is formed, which reacts with CO to form COCl_2 and with CH_4 to form $\text{CH}_{4-n}\text{Cl}_n$. The COCl_2 formation is suggested to occur most likely via stepwise addition of Cl atoms. A second Cl_2 restitutes the reactive $[\text{C}_{60}\cdots\text{Cl}_2]$ species, as the COCl_2 desorbs. The quite marked dependence of the Cl_2 reactions with carbon surfaces of various strain on the sp^2 -hybridized carbons allows us to conclude that COCl_2 synthesis requires carbon catalysts with an intermediate strain to form a sufficient concentration of the critical reversibly bound radical $[\text{C}_{60}\cdots\text{Cl}_2]$ species.

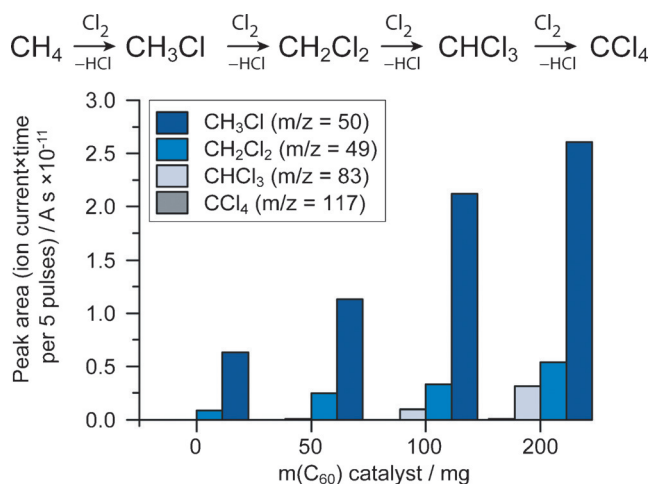


Figure 6. CH₄ chlorination in the absence (0 mg) and in the presence of variable amounts (50–200 mg) of C₆₀ catalyst at 200 °C.

Experimental Section

C₆₀ fullerenes (>99.5%) with a $S_{\text{BET}} < 5 \text{ m}^2 \text{ g}^{-1}$ were purchased from Sigma–Aldrich. C₆₀Cl₃₀ was obtained from Nanofluor GmbH. TEM measurements were performed with a FEI TECNAI 20 electron microscope. The specific surface area and pore volume was determined by N₂ physisorption and Brunauer–Emmett–Teller (BET) using PMI automated Sorptomatic 1990 instrument. ESR spectra were recorded in perpendicular mode on an X-band Joel Jes Fa 200 spectrometer. The measurements were performed in a high-pressure quartz tube at 25 °C (9.45 GHz, 1 mW microwave power). The in situ Raman spectra were measured under isothermal conditions at 40 °C, and the samples were analyzed inside a quartz flow reactor; to maintain Cl₂ atmosphere, Cl₂ containing gas (25% Cl₂ in He, Westfalen) was used. Prior to Cl₂ treatment the samples were activated at 150 °C for 1 h in N₂ flow (99.996%, Westfalen). The Raman spectra at 514.5 nm (2.41 eV, Ar⁺ laser) were taken with Renishaw spectrometer in a backscattering configuration every 43 s. To exclude the possibility of Raman spectral changes that are due to the laser irradiation, the blank test was performed under pure N₂ flow.

The catalytic activity of the carbon materials (≤80 μm particle size) was tested in a quartz pulse reactor (0.4 cm ID; Supporting Information, Figure S2). A six-port valve was used for the automated dosage of Cl₂. C₆₀ was packed in a quartz tube reactor and thermally treated under inert conditions (150 °C, temperature ramp: 5 °C min^{−1}, 10 cm³ s^{−1} He flow; 99.996% He, Westfalen) during 1.0 h prior to measurements. Cl₂ pulses, 60 μL each, (Cl₂ >99.996%, Westfalen) were performed at intervals of 230 s, under atmospheric pressure. The gaseous products were characterized in situ by MS using a PFEIFFER OmniStar quadrupole mass spectrometer (QMS 200). For testing the reactivity of activated Cl₂ at 200 °C, pre-mixed 5% CO and 5% CH₄ in He (>99.9%, Westfalen) were used. The rate of COCl₂ formation was evaluated at a temperature range of 100–350 °C. The Cl₂ and COCl₂ containing gaseous residue was decomposed in two interconnected KOH containing bottles. An active carbon filter finally retained reactive components from the exiting stream.

DFT calculations were carried out using the B3LYP exchange–correlation functional as implemented in Gaussian 09 D.01.^[15] Dispersion interactions were accounted with the D3 version of Grimme's dispersion with Becke–Johnson damping.^[16] Full geometry optimizations were carried out using the 6-31G(d,p) basis set. The energies obtained at this step were further refined by single-point electronic energies computed using the larger TZVP basis set.^[17] Reaction enthalpies were calculated by correcting the electronic energies for zero-point energies and finite temperature contributions calculated from the results of the normal mode analysis at 298.15 K and 1 atm.

The accuracy of the selected method is confirmed by a close agreement between the computed and experimental energetics.

Acknowledgements

The research leading to these results has received funding from the European Community's Seventh Framework Program [FP7/2007–2013] under grant agreement no. NMP-LA-2010-245988 (INCAS). SurfSARA and NWO are acknowledged for providing access to supercomputer resources. The authors thank Dr. Christian Diedrich (BTS) and Dr. Weiyu Song (TU/e) for the discussions and their scientific support.

Keywords: chlorine · density functional calculations · fullerenes · phosgene · reaction mechanisms

How to cite: *Angew. Chem. Int. Ed.* **2016**, *55*, 1728–1732

Angew. Chem. **2016**, *128*, 1760–1764

- a) W. Schneider, W. Diller, *Phosgene, Ullmann's Encyclopedia of Industrial Chemistry*, Weinheim, Wiley-VCH **2005**; b) K. L. Dunlap, *Phosgene, Kirk-Othmer Encyclopedia of Chemical Technology*, John Wiley & Sons, Inc, Hoboken, New Jersey, **2010**, pp. 1–13; c) T. A. Ryan, E. A. Seddon, K. R. Seddon, C. Ryan, *Top. Inorg. Gen. Chem.* **1996**, *24*, 3–932; d) <http://www.phosgenesafety.info>, accessible after registration by the International Isocyanate Institute (III) in Manchester, GB; e) NIST Chemistry WebBook, accessed 16.04.2015, <http://webbook.nist.gov>.
- T. A. Ryan, E. A. Seddon, K. R. Seddon, C. Ryan, *Top. Inorg. Gen. Chem.* **1996**, *24*, 167–220.
- a) C. J. Mitchell, W. v. d. Borden, K. v. d. Velde, M. Smit, R. Scheringa, K. Ahrikas, D. H. Jonesa, *Catal. Sci. Technol.* **2012**, *2*, 2109–2115; b) C. Potter, S. Baron, *Chem. Eng. Prog.* **1951**, *47*, 473–479; c) Z. Csürös, R. Soós, I. Petneházy, G. T. Szabó, *Period. Polytech. Chem. Eng.* **1970**, *14*, 3–11; d) E. N. Shapatina, V. L. Kuchaev, M. I. Temkin, *Kinet. Catal.* **1977**, *18*, 968–972; e) E. N. Shapatina, V. L. Kuchaev, M. I. Temkin, *Kinet. Catal.* **1978**, *19*, 972–976.
- P. Serp, J. L. Figueiredo, *Carbon Materials for Catalysis*, John Wiley & Sons, Inc, Hoboken, New Jersey, **2009**.
- a) A. J. Stone, D. J. Wales, *Chem. Phys. Lett.* **1986**, *128*, 501–503; b) P. A. Thrower, *Chem. Phys. Carbon* **1969**, *5*, 217–320.
- J. Sloan, R. E. Dunin-Borkowski, J. L. Hutchison, K. S. Coleman, V. C. Williams, J. B. Claridge, A. P. E. York, C. Xu, S. R. Bailey, G. Brown, S. Friedrichs, M. L. H. Green, *Chem. Phys. Lett.* **2000**, *316*, 191–198.
- A. Goel, J. B. Howard, J. B. Vander Sande, *Carbon* **2004**, *42*, 1907–1915.
- F. N. Tebbe, J. Y. Becker, D. B. Chase, L. E. Firment, E. R. Holler, B. S. Malone, P. J. Krusic, E. Wassermann, *J. Am. Chem. Soc.* **1991**, *113*, 9900–9901.
- H. Kuzmany, M. Matus, B. Burger, J. Winter, *Adv. Mater.* **1994**, *6*, 731–745.
- D. S. Bethune, G. Meijer, W. C. Tang, H. J. Rosen, *Chem. Phys. Lett.* **1990**, *174*, 219–222.
- M. Kalbác, L. Kavan, M. Zúkalová, L. Dunsch, *Small* **2007**, *3*, 1746–1752.
- a) N. G. Spitsina, M. V. Motyakin, I. V. Bashkin, K. P. Meletov, *J. Phys. Condens. Matter* **2002**, *14*, 11089–11092; b) A. I. Mikhaylov, V. A. Pakhomova, S. I. Kuzina, S. A. Baskakov, Y. M. Shul'ga, A. A. Volodin, V. E. Muradyan, *Nato Sci. Ser. II, Math.* **2007**, 155–158; c) L. Khachatryan, B. Dellinger, *Chemosphere* **2003**, *52*, 709–716; d) M. S. Dresselhaus, G. Dresselhaus,

- P. C. Eklund, *Science of Fullerenes and Carbon Nanotubes: Their Properties and Applications*. Elsevier Science (USA), **1996**.
- [13] M. G. Giuffreda, F. Negri, G. Orlandi, *J. Phys. Chem. A* **2001**, *105*, 9123–9129.
- [14] R. Deng, M. Treat, O. Echt, K. Hansen, *J. Chem. Phys.* **2003**, *118*, 8563–8565.
- [15] Gaussian09 (Revision D.01), M. J. Frisch, Gaussian, Inc., Wallingford CT, **2009** (full reference is given in the Supporting Information).
- [16] S. Grimme, S. Ehrlich, L. Goerigk, *J. Comput. Chem.* **2011**, *32*, 1456–1465.
- [17] a) A. Schäfer, H. Horn, R. Ahlrichs, *J. Chem. Phys.* **1992**, *97*, 2571–2577; b) A. Schäfer, C. Huber, R. Ahlrichs, *J. Chem. Phys.* **1994**, *100*, 5829–5835.

Received: September 23, 2015

Published online: January 6, 2016